

Measurement of $\sigma_{\chi_{c2}} \mathcal{B}(\chi_{c2} \rightarrow J/\psi \gamma) / \sigma_{\chi_{c1}} \mathcal{B}(\chi_{c1} \rightarrow J/\psi \gamma)$ in $p\bar{p}$ Collisions at $\sqrt{s} = 1.96$ TeV

- A. Abulencia,²⁴ J. Adelman,¹³ T. Affolder,¹⁰ T. Akimoto,⁵⁶ M.G. Albrow,¹⁷ D. Ambrose,¹⁷ S. Amerio,⁴⁴
D. Amidei,³⁵ A. Anastassov,⁵³ K. Anikeev,¹⁷ A. Annovi,¹⁹ J. Antos,¹⁴ M. Aoki,⁵⁶ G. Apollinari,¹⁷ J.-F. Arguin,³⁴
T. Arisawa,⁵⁸ A. Artikov,¹⁵ W. Ashmanskas,¹⁷ A. Attal,⁸ F. Azfar,⁴³ P. Azzi-Bacchetta,⁴⁴ P. Azzurri,⁴⁷
N. Bacchetta,⁴⁴ W. Badgett,¹⁷ A. Barbaro-Galtieri,²⁹ V.E. Barnes,⁴⁹ B.A. Barnett,²⁵ S. Baroiant,⁷ V. Bartsch,³¹
G. Bauer,³³ F. Bedeschi,⁴⁷ S. Behari,²⁵ S. Belforte,⁵⁵ G. Bellettini,⁴⁷ J. Bellinger,⁶⁰ A. Belloni,³³ D. Benjamin,¹⁶
A. Beretvas,¹⁷ J. Beringer,²⁹ T. Berry,³⁰ A. Bhatti,⁵¹ M. Binkley,¹⁷ D. Bisello,⁴⁴ R.E. Blair,² C. Blocker,⁶
B. Blumenfeld,²⁵ A. Bocci,¹⁶ A. Bodek,⁵⁰ V. Boisvert,⁵⁰ G. Bolla,⁴⁹ A. Bolshov,³³ D. Bortoletto,⁴⁹ J. Boudreau,⁴⁸
A. Boveia,¹⁰ B. Brau,¹⁰ L. Brigliadori,⁵ C. Bromberg,³⁶ E. Brubaker,¹³ J. Budagov,¹⁵ H.S. Budd,⁵⁰ S. Budd,²⁴
S. Budroni,⁴⁷ K. Burkett,¹⁷ G. Busetto,⁴⁴ P. Bussey,²¹ K. L. Byrum,² S. Cabrera^o,¹⁶ M. Campanelli,²⁰
M. Campbell,³⁵ F. Canelli,¹⁷ A. Canepa,⁴⁹ S. Carilloⁱ,¹⁸ D. Carlsmith,⁶⁰ R. Carosi,⁴⁷ S. Carron,³⁴ M. Casarsa,⁵⁵
A. Castro,⁵ P. Catastini,⁴⁷ D. Cauz,⁵⁵ M. Cavalli-Sforza,³ A. Cerri,²⁹ L. Cerrito^m,⁴³ S.H. Chang,²⁸ Y.C. Chen,¹
M. Chertok,⁷ G. Chiarelli,⁴⁷ G. Chlachidze,¹⁵ F. Chlebana,¹⁷ I. Cho,²⁸ K. Cho,²⁸ D. Chokheli,¹⁵ J.P. Chou,²²
G. Choudalakis,³³ S.H. Chuang,⁶⁰ K. Chung,¹² W.H. Chung,⁶⁰ Y.S. Chung,⁵⁰ M. Ciljak,⁴⁷ C.I. Ciobanu,²⁴
M.A. Ciocci,⁴⁷ A. Clark,²⁰ D. Clark,⁶ M. Coca,¹⁶ G. Compostella,⁴⁴ M.E. Convery,⁵¹ J. Conway,⁷ B. Cooper,³⁶
K. Copic,³⁵ M. Cordelli,¹⁹ G. Cortiana,⁴⁴ F. Crescioli,⁴⁷ C. Cuenca Almenar^o,⁷ J. Cuevas^l,¹¹ R. Culbertson,¹⁷
J.C. Cully,³⁵ D. Cyr,⁶⁰ S. DaRonco,⁴⁴ M. Datta,¹⁷ S. D'Auria,²¹ T. Davies,²¹ M. D'Onofrio,³ D. Dagenhart,⁶
P. de Barbaro,⁵⁰ S. De Cecco,⁵² A. Deisher,²⁹ G. De Lentdecker^c,⁵⁰ M. Dell'Orso,⁴⁷ F. Delli Paoli,⁴⁴ L. Demortier,⁵¹
J. Deng,¹⁶ M. Deninno,⁵ D. De Pedis,⁵² P.F. Derwent,¹⁷ G.P. Di Giovanni,⁴⁵ C. Dionisi,⁵² B. Di Ruzza,⁵⁵
J.R. Dittmann,⁴ P. DiTuro,⁵³ C. Dörr,²⁶ S. Donati,⁴⁷ M. Donega,²⁰ P. Dong,⁸ J. Donini,⁴⁴ T. Dorigo,⁴⁴
S. Dube,⁵³ J. Efron,⁴⁰ R. Erbacher,⁷ D. Errede,²⁴ S. Errede,²⁴ R. Eusebi,¹⁷ H.C. Fang,²⁹ S. Farrington,³⁰
I. Fedorko,⁴⁷ W.T. Fedorko,¹³ R.G. Feild,⁶¹ M. Feindt,²⁶ J.P. Fernandez,³² R. Field,¹⁸ G. Flanagan,⁴⁹ A. Foland,²²
S. Forrester,⁷ G.W. Foster,¹⁷ M. Franklin,²² J.C. Freeman,²⁹ I. Furic,¹³ M. Gallinaro,⁵¹ J. Galyardt,¹² J.E. Garcia,⁴⁷
F. Garberson,¹⁰ A.F. Garfinkel,⁴⁹ C. Gay,⁶¹ H. Gerberich,²⁴ D. Gerdes,³⁵ S. Giagu,⁵² P. Giannetti,⁴⁷ A. Gibson,²⁹
K. Gibson,⁴⁸ J.L. Gimmell,⁵⁰ C. Ginsburg,¹⁷ N. Giokaris^a,¹⁵ M. Giordani,⁵⁵ P. Giromini,¹⁹ M. Giunta,⁴⁷
G. Giurgiu,¹² V. Glagolev,¹⁵ D. Glenzinski,¹⁷ M. Gold,³⁸ N. Goldschmidt,¹⁸ J. Goldstein^b,⁴³ A. Golossanov,¹⁷
G. Gomez,¹¹ G. Gomez-Ceballos,¹¹ M. Goncharov,⁵⁴ O. Gonzalez,³² I. Gorelov,³⁸ A.T. Goshaw,¹⁶
K. Goulianatos,⁵¹ A. Gresele,⁴⁴ M. Griffiths,³⁰ S. Grinstein,²² C. Grossi-Pilcher,¹³ R.C. Group,¹⁸ U. Grundler,²⁴
J. Guimaraes da Costa,²² Z. Gunay-Unalan,³⁶ C. Haber,²⁹ K. Hahn,³³ S.R. Hahn,¹⁷ E. Halkiadakis,⁵³
A. Hamilton,³⁴ B.-Y. Han,⁵⁰ J.Y. Han,⁵⁰ R. Handler,⁶⁰ F. Happacher,¹⁹ K. Hara,⁵⁶ M. Hare,⁵⁷ S. Harper,⁴³
R.F. Harr,⁵⁹ R.M. Harris,¹⁷ M. Hartz,⁴⁸ K. Hatakeyama,⁵¹ J. Hauser,⁸ A. Heijboer,⁴⁶ B. Heinemann,³⁰
J. Heinrich,⁴⁶ C. Henderson,³³ M. Herndon,⁶⁰ J. Heuser,²⁶ D. Hidas,¹⁶ C.S. Hill^b,¹⁰ D. Hirschbuehl,²⁶ A. Hocker,¹⁷
A. Holloway,²² S. Hou,¹ M. Houlden,³⁰ S.-C. Hsu,⁹ B.T. Huffman,⁴³ R.E. Hughes,⁴⁰ U. Husemann,⁶¹
J. Huston,³⁶ J. Incandela,¹⁰ G. Introzzi,⁴⁷ M. Iori,⁵² Y. Ishizawa,⁵⁶ A. Ivanov,⁷ B. Iyutin,³³ E. James,¹⁷
D. Jang,⁵³ B. Jayatilaka,³⁵ D. Jeans,⁵² H. Jensen,¹⁷ E.J. Jeon,²⁸ S. Jindariani,¹⁸ M. Jones,⁴⁹ K.K. Joo,²⁸
S.Y. Jun,¹² J.E. Jung,²⁸ T.R. Junk,²⁴ T. Kamon,⁵⁴ P.E. Karchin,⁵⁹ Y. Kato,⁴² Y. Kemp,²⁶ R. Kephart,¹⁷
U. Kerzel,²⁶ V. Khotilovich,⁵⁴ B. Kilminster,⁴⁰ D.H. Kim,²⁸ H.S. Kim,²⁸ J.E. Kim,²⁸ M.J. Kim,¹² S.B. Kim,²⁸
S.H. Kim,⁵⁶ Y.K. Kim,¹³ N. Kimura,⁵⁶ L. Kirsch,⁶ S. Klimentko,¹⁸ M. Klute,³³ B. Knuteson,³³ B.R. Ko,¹⁶
K. Kondo,⁵⁸ D.J. Kong,²⁸ J. Konigsberg,¹⁸ A. Korytov,¹⁸ A.V. Kotwal,¹⁶ A. Kovalev,⁴⁶ A.C. Kraan,⁴⁶ J. Kraus,²⁴
I. Kravchenko,³³ M. Kreps,²⁶ J. Kroll,⁴⁶ N. Krumnack,⁴ M. Kruse,¹⁶ V. Krutelyov,¹⁰ T. Kubo,⁵⁶ S. E. Kuhlmann,²
T. Kuhr,²⁶ Y. Kusakabe,⁵⁸ S. Kwang,¹³ A.T. Laasanen,⁴⁹ S. Lai,³⁴ S. Lami,⁴⁷ S. Lammel,¹⁷ M. Lancaster,³¹
R.L. Lander,⁷ K. Lannon,⁴⁰ A. Lath,⁵³ G. Latino,⁴⁷ I. Lazzizzera,⁴⁴ T. LeCompte,² J. Lee,⁵⁰ J. Lee,²⁸ Y.J. Lee,²⁸
S.W. Leeⁿ,⁵⁴ R. Lefevre,³ N. Leonardo,³³ S. Leone,⁴⁷ S. Levy,¹³ J.D. Lewis,¹⁷ C. Lin,⁶¹ C.S. Lin,¹⁷ M. Lindgren,¹⁷
E. Lipeles,⁹ A. Lister,⁷ D.O. Litvintsev,¹⁷ T. Liu,¹⁷ N.S. Lockyer,⁴⁶ A. Loginov,⁶¹ M. Loretta,⁴⁴ P. Loverre,⁵²
R.-S. Lu,¹ D. Lucchesi,⁴⁴ P. Lujan,²⁹ P. Lukens,¹⁷ G. Lungu,¹⁸ L. Lyons,⁴³ J. Lys,²⁹ R. Lysak,¹⁴ E. Lytken,⁴⁹
P. Mack,²⁶ D. MacQueen,³⁴ R. Madrak,¹⁷ K. Maeshima,¹⁷ K. Makhoul,³³ T. Maki,²³ P. Maksimovic,²⁵ S. Malde,⁴³
G. Manca,³⁰ F. Margaroli,⁵ R. Marginean,¹⁷ C. Marino,²⁶ C.P. Marino,²⁴ A. Martin,⁶¹ M. Martin,²⁵ V. Martin^g,²¹
M. Martínez,³ T. Maruyama,⁵⁶ P. Mastrandrea,⁵² T. Masubuchi,⁵⁶ H. Matsunaga,⁵⁶ M.E. Mattson,⁵⁹ R. Mazini,³⁴
P. Mazzanti,⁵ K.S. McFarland,⁵⁰ P. McIntyre,⁵⁴ R. McNulty^f,³⁰ A. Mehta,³⁰ P. Mehtala,²³ S. Menzemer^h,¹¹
A. Menzione,⁴⁷ P. Merkel,⁴⁹ C. Mesropian,⁵¹ A. Messina,³⁶ T. Miao,¹⁷ N. Miladinovic,⁶ J. Miles,³³ R. Miller,³⁶
C. Mills,¹⁰ M. Milnik,²⁶ A. Mitra,¹ G. Mitselmakher,¹⁸ A. Miyamoto,²⁷ S. Moed,²⁰ N. Moggi,⁵ B. Mohr,⁸
R. Moore,¹⁷ M. Morello,⁴⁷ P. Movilla Fernandez,²⁹ J. Müllenstädt,²⁹ A. Mukherjee,¹⁷ Th. Muller,²⁶ R. Mumford,²⁵
P. Murat,¹⁷ J. Nachtman,¹⁷ A. Nagano,⁵⁶ J. Naganoma,⁵⁸ I. Nakano,⁴¹ A. Napier,⁵⁷ V. Necula,¹⁸ C. Neu,⁴⁶

M.S. Neubauer,⁹ J. Nielsen,²⁹ T. Nigmanov,⁴⁸ L. Nodulman,² O. Norniella,³ E. Nurse,³¹ S.H. Oh,¹⁶ Y.D. Oh,²⁸ I. Oksuzian,¹⁸ T. Okusawa,⁴² R. Oldeman,³⁰ R. Orava,²³ K. Osterberg,²³ C. Pagliarone,⁴⁷ E. Palencia,¹¹ V. Papadimitriou,¹⁷ A.A. Paramonov,¹³ B. Parks,⁴⁰ S. Pashapour,³⁴ J. Patrick,¹⁷ G. Paulette,⁵⁵ M. Paulini,¹² C. Paus,³³ D.E. Pellett,⁷ A. Penzo,⁵⁵ T.J. Phillips,¹⁶ G. Piacentino,⁴⁷ J. Piedra,⁴⁵ L. Pinera,¹⁸ K. Pitts,²⁴ C. Plager,⁸ L. Pondrom,⁶⁰ X. Portell,³ O. Poukhov,¹⁵ N. Pounder,⁴³ F. Prakoshyn,¹⁵ A. Pronko,¹⁷ J. Proudfoot,² F. Ptohos^e,¹⁹ G. Punzi,⁴⁷ J. Pursley,²⁵ J. Rademacker^b,⁴³ A. Rahaman,⁴⁸ N. Ranjan,⁴⁹ S. Rappoccio,²² B. Reisert,¹⁷ V. Rekovic,³⁸ P. Renton,⁴³ M. Rescigno,⁵² S. Richter,²⁶ F. Rimondi,⁵ L. Ristori,⁴⁷ A. Robson,²¹ T. Rodrigo,¹¹ E. Rogers,²⁴ S. Rolli,⁵⁷ R. Roser,¹⁷ M. Rossi,⁵⁵ R. Rossin,¹⁸ A. Ruiz,¹¹ J. Russ,¹² V. Rusu,¹³ H. Saarikko,²³ S. Sabik,³⁴ A. Safonov,⁵⁴ W.K. Sakumoto,⁵⁰ G. Salamanna,⁵² O. Saltó,³ D. Saltzberg,⁸ C. Sánchez,³ L. Santi,⁵⁵ S. Sarkar,⁵² L. Sartori,⁴⁷ K. Sato,¹⁷ P. Savard,³⁴ A. Savoy-Navarro,⁴⁵ T. Scheidle,²⁶ P. Schlabach,¹⁷ E.E. Schmidt,¹⁷ M.P. Schmidt,⁶¹ M. Schmitt,³⁹ T. Schwarz,⁷ L. Scodellaro,¹¹ A.L. Scott,¹⁰ A. Scribano,⁴⁷ F. Scuri,⁴⁷ A. Sedov,⁴⁹ S. Seidel,³⁸ Y. Seiya,⁴² A. Semenov,¹⁵ L. Sexton-Kennedy,¹⁷ A. Sfyrla,²⁰ M.D. Shapiro,²⁹ T. Shears,³⁰ P.F. Shepard,⁴⁸ D. Sherman,²² M. Shimojima^k,⁵⁶ M. Shochet,¹³ Y. Shon,⁶⁰ I. Shreyber,³⁷ A. Sidoti,⁴⁷ P. Sinervo,³⁴ A. Sisakyan,¹⁵ J. Sjolin,⁴³ A.J. Slaughter,¹⁷ J. Slaunwhite,⁴⁰ K. Sliwa,⁵⁷ J.R. Smith,⁷ F.D. Snider,¹⁷ R. Snihur,³⁴ M. Soderberg,³⁵ A. Soha,⁷ S. Somalwar,⁵³ V. Sorin,³⁶ J. Spalding,¹⁷ F. Spinella,⁴⁷ T. Spreitzer,³⁴ P. Squillacioti,⁴⁷ M. Stanitzki,⁶¹ A. Staveris-Polykalas,⁴⁷ R. St. Denis,²¹ B. Stelzer,⁸ O. Stelzer-Chilton,⁴³ D. Stentz,³⁹ J. Strologas,³⁸ D. Stuart,¹⁰ J.S. Suh,²⁸ A. Sukhanov,¹⁸ H. Sun,⁵⁷ T. Suzuki,⁵⁶ A. Taffard,²⁴ R. Takashima,⁴¹ Y. Takeuchi,⁵⁶ K. Takikawa,⁵⁶ M. Tanaka,² R. Tanaka,⁴¹ M. Tecchio,³⁵ P.K. Teng,¹ K. Terashi,⁵¹ J. Thom^d,¹⁷ A.S. Thompson,²¹ E. Thomson,⁴⁶ P. Tipton,⁶¹ V. Tiwari,¹² S. Tkaczyk,¹⁷ D. Toback,⁵⁴ S. Tokar,¹⁴ K. Tollefson,³⁶ T. Tomura,⁵⁶ D. Tonelli,⁴⁷ S. Torre,¹⁹ D. Torretta,¹⁷ S. Tourneur,⁴⁵ W. Trischuk,³⁴ R. Tsuchiya,⁵⁸ S. Tsuno,⁴¹ N. Turini,⁴⁷ F. Ukegawa,⁵⁶ T. Unverhau,²¹ S. Uozumi,⁵⁶ D. Usynin,⁴⁶ S. Vallecorsa,²⁰ N. van Remortel,²³ A. Varganov,³⁵ E. Vataga,³⁸ F. Vázquezⁱ,¹⁸ G. Velev,¹⁷ G. Veramendi,²⁴ V. Vespremi,⁴⁹ R. Vidal,¹⁷ I. Vila,¹¹ R. Vilar,¹¹ T. Vine,³¹ I. Vollrath,³⁴ I. Volobouevⁿ,²⁹ G. Volpi,⁴⁷ F. Würthwein,⁹ P. Wagner,⁵⁴ R.G. Wagner,² R.L. Wagner,¹⁷ J. Wagner,²⁶ W. Wagner,²⁶ R. Wallny,⁸ S.M. Wang,¹ A. Warburton,³⁴ S. Waschke,²¹ D. Waters,³¹ M. Weinberger,⁵⁴ W.C. Wester III,¹⁷ B. Whitehouse,⁵⁷ D. Whiteson,⁴⁶ A.B. Wicklund,² E. Wicklund,¹⁷ G. Williams,³⁴ H.H. Williams,⁴⁶ P. Wilson,¹⁷ B.L. Winer,⁴⁰ P. Wittich^d,¹⁷ S. Wolbers,¹⁷ C. Wolfe,¹³ T. Wright,³⁵ X. Wu,²⁰ S.M. Wynne,³⁰ A. Yagil,¹⁷ K. Yamamoto,⁴² J. Yamaoka,⁵³ T. Yamashita,⁴¹ C. Yang,⁶¹ U.K. Yang^j,¹³ Y.C. Yang,²⁸ W.M. Yao,²⁹ G.P. Yeh,¹⁷ J. Yoh,¹⁷ K. Yorita,¹³ T. Yoshida,⁴² G.B. Yu,⁵⁰ I. Yu,²⁸ S.S. Yu,¹⁷ J.C. Yun,¹⁷ L. Zanello,⁵² A. Zanetti,⁵⁵ I. Zaw,²² X. Zhang,²⁴ J. Zhou,⁵³ and S. Zucchelli⁵

(CDF Collaboration*)

¹*Institute of Physics, Academia Sinica, Taipei, Taiwan 11529, Republic of China*

²*Argonne National Laboratory, Argonne, Illinois 60439*

³*Institut de Fisica d'Altes Energies, Universitat Autònoma de Barcelona, E-08193, Bellaterra (Barcelona), Spain*

⁴*Baylor University, Waco, Texas 76798*

⁵*Istituto Nazionale di Fisica Nucleare, University of Bologna, I-40127 Bologna, Italy*

⁶*Brandeis University, Waltham, Massachusetts 02254*

⁷*University of California, Davis, Davis, California 95616*

⁸*University of California, Los Angeles, Los Angeles, California 90024*

⁹*University of California, San Diego, La Jolla, California 92093*

¹⁰*University of California, Santa Barbara, Santa Barbara, California 93106*

¹¹*Instituto de Fisica de Cantabria, CSIC-University of Cantabria, 39005 Santander, Spain*

¹²*Carnegie Mellon University, Pittsburgh, PA 15213*

¹³*Enrico Fermi Institute, University of Chicago, Chicago, Illinois 60637*

¹⁴*Comenius University, 842 48 Bratislava, Slovakia; Institute of Experimental Physics, 040 01 Kosice, Slovakia*

¹⁵*Joint Institute for Nuclear Research, RU-141980 Dubna, Russia*

¹⁶*Duke University, Durham, North Carolina 27708*

¹⁷*Fermi National Accelerator Laboratory, Batavia, Illinois 60510*

¹⁸*University of Florida, Gainesville, Florida 32611*

¹⁹*Laboratori Nazionali di Frascati, Istituto Nazionale di Fisica Nucleare, I-00044 Frascati, Italy*

²⁰*University of Geneva, CH-1211 Geneva 4, Switzerland*

²¹*Glasgow University, Glasgow G12 8QQ, United Kingdom*

²²*Harvard University, Cambridge, Massachusetts 02138*

²³*Division of High Energy Physics, Department of Physics, University of Helsinki and Helsinki Institute of Physics, FIN-00014, Helsinki, Finland*

²⁴*University of Illinois, Urbana, Illinois 61801*

²⁵*The Johns Hopkins University, Baltimore, Maryland 21218*

²⁶*Institut für Experimentelle Kernphysik, Universität Karlsruhe, 76128 Karlsruhe, Germany*

²⁷*High Energy Accelerator Research Organization (KEK), Tsukuba, Ibaraki 305, Japan*

- ²⁸Center for High Energy Physics: Kyungpook National University, Taegu 702-701, Korea; Seoul National University, Seoul 151-742, Korea; and SungKyunKwan University, Suwon 440-746, Korea
- ²⁹Ernest Orlando Lawrence Berkeley National Laboratory, Berkeley, California 94720
- ³⁰University of Liverpool, Liverpool L69 7ZE, United Kingdom
- ³¹University College London, London WC1E 6BT, United Kingdom
- ³²Centro de Investigaciones Energeticas Medioambientales y Tecnologicas, E-28040 Madrid, Spain
- ³³Massachusetts Institute of Technology, Cambridge, Massachusetts 02139
- ³⁴Institute of Particle Physics: McGill University, Montréal, Canada H3A 2T8; and University of Toronto, Toronto, Canada M5S 1A7
- ³⁵University of Michigan, Ann Arbor, Michigan 48109
- ³⁶Michigan State University, East Lansing, Michigan 48824
- ³⁷Institution for Theoretical and Experimental Physics, ITEP, Moscow 117259, Russia
- ³⁸University of New Mexico, Albuquerque, New Mexico 87131
- ³⁹Northwestern University, Evanston, Illinois 60208
- ⁴⁰The Ohio State University, Columbus, Ohio 43210
- ⁴¹Okayama University, Okayama 700-8530, Japan
- ⁴²Osaka City University, Osaka 588, Japan
- ⁴³University of Oxford, Oxford OX1 3RH, United Kingdom
- ⁴⁴University of Padova, Istituto Nazionale di Fisica Nucleare, Sezione di Padova-Trento, I-35131 Padova, Italy
- ⁴⁵LPNHE, Université Pierre et Marie Curie/IN2P3-CNRS, UMR7585, Paris, F-75252 France
- ⁴⁶University of Pennsylvania, Philadelphia, Pennsylvania 19104
- ⁴⁷Istituto Nazionale di Fisica Nucleare Pisa, Universities of Pisa, Siena and Scuola Normale Superiore, I-56127 Pisa, Italy
- ⁴⁸University of Pittsburgh, Pittsburgh, Pennsylvania 15260
- ⁴⁹Purdue University, West Lafayette, Indiana 47907
- ⁵⁰University of Rochester, Rochester, New York 14627
- ⁵¹The Rockefeller University, New York, New York 10021
- ⁵²Istituto Nazionale di Fisica Nucleare, Sezione di Roma 1, University of Rome "La Sapienza," I-00185 Roma, Italy
- ⁵³Rutgers University, Piscataway, New Jersey 08855
- ⁵⁴Texas A&M University, College Station, Texas 77843
- ⁵⁵Istituto Nazionale di Fisica Nucleare, University of Trieste/ Udine, Italy
- ⁵⁶University of Tsukuba, Tsukuba, Ibaraki 305, Japan
- ⁵⁷Tufts University, Medford, Massachusetts 02155
- ⁵⁸Waseda University, Tokyo 169, Japan
- ⁵⁹Wayne State University, Detroit, Michigan 48201
- ⁶⁰University of Wisconsin, Madison, Wisconsin 53706
- ⁶¹Yale University, New Haven, Connecticut 06520

We measure the ratio of cross section times branching fraction, $R_p \equiv \sigma_{\chi_{c2}} \mathcal{B}(\chi_{c2} \rightarrow J/\psi \gamma) / \sigma_{\chi_{c1}} \mathcal{B}(\chi_{c1} \rightarrow J/\psi \gamma)$, in 1.1 fb^{-1} of $p\bar{p}$ collisions at $\sqrt{s} = 1.96 \text{ TeV}$. This measurement covers the kinematic range $p_T(J/\psi) > 4.0 \text{ GeV}/c$, $|\eta(J/\psi)| < 1.0$, and $p_T(\gamma) > 1.0 \text{ GeV}/c$. For events due to prompt processes, we find $R_p = 0.395 \pm 0.016(\text{stat.}) \pm 0.015(\text{sys.})$. This result represents a significant improvement in precision over previous measurements of prompt $\chi_{c1,2}$ hadroproduction.

PACS numbers: 13.60Le, 13.85Qk

Since it was first observed, charmonium ($c\bar{c}$) production in hadronic collisions has been a subject of considerable theoretical interest. Recent approaches to under-

standing charmonium production make use of nonrelativistic QCD [1, 2] to calculate hadro-production rates at the Tevatron and elsewhere. While most experimental observations of charmonium production consist of J/ψ measurements, a significant contribution of J/ψ production is indirect, resulting from the decay of higher mass states [3]. In particular, the radiative decay of the χ_{cJ} states [4] accounts for a significant fraction of the J/ψ production seen in hadronic collisions, and any calculation of J/ψ production must include χ_{cJ} production as well.

Measurements of hadronic χ_{cJ} production have been made in a variety of beam types and energies [5] by ob-

*With visitors from ^aUniversity of Athens, ^bUniversity of Bristol, ^cUniversity Libre de Bruxelles, ^dCornell University, ^eUniversity of Cyprus, ^fUniversity of Dublin, ^gUniversity of Edinburgh, ^hUniversity of Heidelberg, ⁱUniversidad Iberoamericana, ^jUniversity of Manchester, ^kNagasaki Institute of Applied Science, ^lUniversity de Oviedo, ^mUniversity of London, Queen Mary and Westfield College, ⁿTexas Tech University, ^oIFIC(CSIC-Universitat de València),

serving the decay process $\chi_{cJ} \rightarrow J/\psi\gamma$. Experimental results available until now have suffered from large statistical uncertainties, and no measurement has had the precision to test the consistency of the cross-section ratio $\sigma_{\chi_{c2}}/\sigma_{\chi_{c1}}$ with the simple spin-state counting expectation of $\frac{5}{3}$ for χ_{cJ} mesons that are directly produced in the interaction [6]. Knowledge of this ratio is needed in calculations of J/ψ production through radiative χ_{cJ} decay, and can be an important standard for comparing production models.

In this letter, we report a measurement of the relative cross section times branching fractions of the χ_{c1} and χ_{c2} mesons produced in $p\bar{p}$ collisions at a center of mass energy of 1.96 TeV using the CDF II detector at the Fermilab Tevatron. We study the inclusive process $p\bar{p} \rightarrow \chi_{cJ}X$, where $\chi_{cJ} \rightarrow J/\psi\gamma$, and $J/\psi \rightarrow \mu^+\mu^-$, in a data sample with a time-integrated luminosity of 1.1 fb^{-1} . The final state photon is reconstructed through its conversion into e^+e^- , which provides the mass resolution needed to distinguish the χ_{c1} and χ_{c2} states. The spatial resolution of the $\mu^+\mu^-$ vertex allows separation of prompt χ_{cJ} production from events where the χ_{cJ} meson is a B -hadron decay product. We measure the ratio of the cross section times branching fraction $R_p \equiv \sigma_{\chi_{c2}}\mathcal{B}(\chi_{c2} \rightarrow J/\psi\gamma)/\sigma_{\chi_{c1}}\mathcal{B}(\chi_{c1} \rightarrow J/\psi\gamma)$ for promptly produced χ_{cJ} mesons. In addition, we obtain a result for the analogous quantity in B decay events, $R_B \equiv \sigma_B\mathcal{B}(B \rightarrow \chi_{c2}X)\mathcal{B}(\chi_{c2} \rightarrow J/\psi\gamma)/\sigma_B\mathcal{B}(B \rightarrow \chi_{c1}X)\mathcal{B}(\chi_{c1} \rightarrow J/\psi\gamma)$, which provides a measurement of $\mathcal{B}(B \rightarrow \chi_{c2}X)/\mathcal{B}(B \rightarrow \chi_{c1}X)$ for the B hadrons produced in the Tevatron environment.

This analysis makes use of the tracking, muon identification, and trigger systems. The CDF II detector has been described in detail elsewhere [8, 9]. The tracking system consists of a seven-layer silicon microstrip detector and an open-cell drift chamber (COT) that operate inside a solenoid with a 1.4 T magnetic field. Muon candidates from the decay $J/\psi \rightarrow \mu^+\mu^-$ are identified by two sets of drift chambers located outside the electromagnetic and hadronic calorimeters. The central muon chambers cover the pseudorapidity region $|\eta| < 0.6$, and are sensitive to muons having transverse momentum $p_T > 1.4 \text{ GeV}/c$ [10]. A second muon system covers the region $0.6 < |\eta| < 1.0$ and is sensitive to muons having $p_T > 2.0 \text{ GeV}/c$. Muon triggering and identification are based on matching tracks measured in the muon system to COT tracks.

The analysis of the data begins with a selection of well measured $J/\psi \rightarrow \mu^+\mu^-$ candidates. These are selected by requiring events that contain two oppositely charged muon candidates, each with a match between the COT and muon chamber tracks. We also require that both muon tracks have measurements in at least three layers of the silicon detector and a two-track invariant mass within $\pm 80 \text{ MeV}/c^2$ of the world-average J/ψ mass [7]. The J/ψ candidates are required to fall within kinematic bounds of $p_T(J/\psi) > 4.0 \text{ GeV}/c$ and $|\eta(J/\psi)| < 1.0$, which correspond to the approximate limits of our ac-

ceptance. A simultaneous mass and vertex constrained fit is performed on the muon tracks, where the dimuon mass is constrained to the world-average J/ψ mass.

The search for photon conversion candidates begins with a scan of all additional tracks with $p_T > 400 \text{ MeV}/c$ found in each J/ψ event. Two oppositely charged tracks are each assigned the electron mass, and have their track parameters recalculated by subjecting them and their uncertainties to a fit that has constraints consistent with the photon conversion hypothesis. Specifically, the two tracks are constrained to be parallel at their point of intersection, and the momentum vector of the pair is constrained to originate from the dimuon vertex. A displacement of 12.0 cm or more from the beam line in the direction of the track pair's transverse momentum is required to omit conversions whose momentum is poorly measured due to bremsstrahlung in the inner detector material. We also require $p_T(\gamma) > 1.0 \text{ GeV}/c$. Finally, a constrained fit is performed on the four tracks that combines the J/ψ mass constraint with the photon conversion hypothesis. The invariant mass distribution of all $J/\psi\gamma$ combinations is shown in Fig. 1, which clearly demonstrates that the $J/\psi\gamma$ mass resolution achieved by this technique is sufficient to resolve the χ_{cJ} states.

The lifetime of B hadrons allows the transverse displacement of the dimuon vertex from the beamline to be used as a tool for their identification. Since any $J/\psi\gamma$ combination that originates from B decay represents only a partial reconstruction of the B hadron, the proper lifetime is not directly measurable. We therefore use the quantity $ct \equiv L \times M(J/\psi) \times F(p_T(J/\psi))/p_T(J/\psi)$ where $M(J/\psi)$ and $p_T(J/\psi)$ are the mass and transverse momentum, respectively, of the J/ψ candidate, and L is the measured displacement of the dimuon vertex in the direction of $p_T(J/\psi)$. The correction factor, $F(p_T(J/\psi))$, was obtained by a Monte Carlo simulation of B hadron decay [3], and provides an average correction between the measured displacement and the lifetime of the decaying B hadron.

Mass resolution, acceptance, and reconstruction efficiencies for $J/\psi\gamma$ final states of different invariant mass have been studied with a Monte Carlo simulation that generates events uniformly in rapidity and with a transverse momentum distribution that matches the measured distribution for J/ψ events [8]. The simulated events were processed through our reconstruction and analysis algorithms, and provided templates for the expected signal shape of the final $J/\psi\gamma$ invariant mass distribution as a function of $p_T(J/\psi)$. In particular, the simulated events enabled an estimate of the mass resolution and radiative tail due to scattering and radiation by the conversion electrons as they passed through the material in the detector.

We used an unbinned likelihood fit to calculate the yield of χ_{cJ} events for both prompt and B -decay production processes. The probability density function used for the fit is a function of both $J/\psi\gamma$ invariant mass and ct . Independent signal and background distribu-

tions are calculated for both processes. The mass distributions of the signals are constrained to the templates obtained through simulation. The mass distributions of the backgrounds are modeled by polynomials, and the probability density function for each event uses the calculated uncertainty on the invariant mass and ct . The ct distribution is used to separate the production processes, and is modeled as a sum of prompt (Gaussian resolution) and B -decay (exponential, convoluted with resolution) contributions. Our fit to the data gives an event yield ($N_{\chi_{cJ}}$) of $N_{\chi_{c0}} = 41 \pm 20$, $N_{\chi_{c1}} = 2143 \pm 60$, and $N_{\chi_{c2}} = 1035 \pm 40$ for promptly produced events. For B decay events, the yields are $N_{\chi_{c0}} = 29 \pm 16$, $N_{\chi_{c1}} = 384 \pm 35$, and $N_{\chi_{c2}} = 66 \pm 16$. Projections of the unbinned likelihood fit are overlaid onto the mass and ct distributions shown in Figs. 1 and 2. The relatively small yield of χ_{c0} candidates is due to the small branching fraction into the $J/\psi\gamma$ final state [7], and is the reason they were not used in the subsequent analysis.

For our acceptance calculation, we have analyzed our simulated events assuming every photon converted, and created electron-positron pairs according to the Bethe-Heitler distribution [11]. We then counted the number of events that would have been accepted if all final state products were to pass our kinematic requirements. Our low transverse momentum limit of 400 MeV/ c for the electrons results in a dependence of our acceptance on the invariant mass of the parent. The overall ratio of the χ_{c1} and χ_{c2} meson acceptances ($\epsilon_{\chi_{c2}}/\epsilon_{\chi_{c1}}$) is listed in Table I for several ranges of $p_T(J/\psi)$. The acceptance ratio is then combined with our yield ratios to provide measurements of R_p and R_B for several ranges of $p_T(J/\psi)$.

TABLE I: The acceptance ratio and ratios of cross section times branching fractions of the χ_{cJ} states for the prompt events and B decay events. Uncertainties listed are statistical only.

$p_T(J/\psi)$ (GeV/ c)	$\epsilon_{\chi_{c2}}/\epsilon_{\chi_{c1}}$	R_p	R_B
4 – 6	1.27 ± 0.01	0.457 ± 0.039	0.150 ± 0.087
6 – 8	1.17 ± 0.01	0.384 ± 0.034	0.080 ± 0.094
8 – 10	1.14 ± 0.01	0.455 ± 0.053	0.116 ± 0.070
> 10	1.10 ± 0.01	0.309 ± 0.045	0.197 ± 0.082
> 4	1.23 ± 0.01	0.395 ± 0.016	0.143 ± 0.042

Several systematic effects that might change the reconstruction efficiency ratio $\epsilon_{\chi_{c2}}/\epsilon_{\chi_{c1}}$ were studied. First, the simulated event sample size used for the acceptance calculation provides an overall relative uncertainty of ± 0.005 on the ratio. A comparison between the full event simulation/reconstruction and the simpler simulation based on the electron energy distribution yields a relative systematic uncertainty of ± 0.020 . Another effect considered is that polarization of one of the two χ_{cJ} states would also introduce a systematic shift. We have evaluated the effect of having one state decay with a dis-

tribution given by $I(\theta_{\mu\mu}) \propto 1 + \alpha \cos^2(\theta_{\mu\mu})$ where $\theta_{\mu\mu}$ is the polar angle of the μ^+ in the J/ψ rest frame, and we take $\alpha = 0.13 \pm 0.15$ as was done for a separate J/ψ cross-section measurement [8]. A variation of α by this uncertainty for one of the two χ_{cJ} states implies a relative shift of ± 0.030 on our reconstruction efficiency ratio.

We have also considered the sources of systematic uncertainty in the yield ratio calculation. We varied the invariant mass signal shape obtained from the simulation within the uncertainty of its parametrization, and found that the relative shift in the yield ratio is ± 0.005 . The uncertainty on parameters used in the ct definition corresponds to a variation of the B fraction of the $J/\psi\gamma$ events of ± 0.007 of its value, giving a systematic uncertainty of $\pm 0.002(\pm 0.010)$ in the yield ratio for the prompt(B decay) sample. Finally, we explored the possibility that our data contain partially reconstructed $h_c \rightarrow J/\psi\pi^0$, $\pi^0 \rightarrow \gamma\gamma$ events. This has been studied by simulating this process, parametrizing the resulting $J/\psi\gamma$ invariant mass distribution, and including this possible background in our likelihood fits for the signal yield. The possible h_c background contribution was found to be negligible in this data sample, so no systematic uncertainty was assigned for this process.

Differences in the two states due to production angular or p_T distributions would require different production mechanisms for the χ_{c1} and χ_{c2} mesons, and are, therefore, considered to be unlikely. Consequently, we did not assign a systematic uncertainty on the χ_{cJ} acceptance due to production dynamics. A summary of the systematic uncertainties on the cross section times branching fraction ratio is listed in Table II. The individual uncertainties are combined in quadrature to give the total systematic uncertainty.

TABLE II: Relative systematic uncertainties on R_p and R_B .

Effect	Uncertainty
Simulation Sample Size	± 0.005
Photon Conversion Simulation	± 0.020
Polarization Effects	± 0.030
Invariant Mass Resolution	± 0.005
Prompt/ B Separation	$\pm 0.002(\pm 0.010 \text{ for } B)$
Total	$\pm 0.037 (\pm 0.038 \text{ for } B)$

Our final result on the relative rate of production for promptly produced χ_{cJ} states is $R_p = 0.395 \pm 0.016(\text{stat.}) \pm 0.015(\text{sys.})$ for χ_{cJ} with $p_T(J/\psi) > 4$ GeV/ c and $p_T(\gamma) > 1$ GeV/ c . For χ_{cJ} resulting from B decay over the same kinematic range we find $R_B = 0.143 \pm 0.042(\text{stat.}) \pm 0.005(\text{sys.})$. These results provide the most precise measurement of the χ_{cJ} production ratio obtained in any hadronic interactions. Conversion of this measurement into the direct cross-section ratio $\sigma_{\chi_{c2}}/\sigma_{\chi_{c1}}$ requires a knowledge of the branching fractions, which are not measured in this experiment, and a small correction due to $\psi(2S) \rightarrow \chi_{cJ}\gamma$ decays. Based on the existing

measurement of the prompt $\psi(2S)$ cross section [12], and the χ_{cJ} contribution to the prompt J/ψ production cross section [3], we estimate that 4.0 ± 1.0 (5.0 ± 1.0)% of our prompt $\chi_{c1}(\chi_{c2})$ sample is due to decay of promptly produced $\psi(2S)$ mesons.

Prior measurements of the prompt cross-section ratio have been severely limited in their precision due to the statistical uncertainties inherent to small data samples [5]. The relative precision of previous measurements has typically been approximately 30% on the cross-section ratio, and provides weak guidance for production models. This work, combined with the best branching-fraction ratio measurement $R_{J/\psi\gamma} \equiv \mathcal{B}(\chi_{c1} \rightarrow J/\psi\gamma)/\mathcal{B}(\chi_{c2} \rightarrow J/\psi\gamma) = 1.91 \pm 0.10$ available [13], gives $R_p R_{J/\psi\gamma} = 0.75 \pm 0.03(\text{stat.}) \pm 0.03(\text{sys.}) \pm 0.04(\text{B.F.})$, where the last term in the uncertainty is due to the branching-fraction ratio uncertainty. This level of precision should serve to inform any future developments in the calculation of hadronic charmonium production.

We thank the Fermilab staff and the technical staffs

of the participating institutions for their vital contributions. This work was supported by the U.S. Department of Energy and National Science Foundation; the Italian Istituto Nazionale di Fisica Nucleare; the Ministry of Education, Culture, Sports, Science and Technology of Japan; the Natural Sciences and Engineering Research Council of Canada; the National Science Council of the Republic of China; the Swiss National Science Foundation; the A.P. Sloan Foundation; the Bundesministerium für Bildung und Forschung, Germany; the Korean Science and Engineering Foundation and the Korean Research Foundation; the Particle Physics and Astronomy Research Council and the Royal Society, UK; the Institut National de Physique Nucléaire et Physique des Particules/CNRS; the Russian Foundation for Basic Research; the Comisión Interministerial de Ciencia y Tecnología, Spain; in part by the European Community's Human Potential Programme under contract HPRN-CT-2002-00292; and the Academy of Finland.

-
- [1] G.T. Bodwin, E. Braaten, and J. Lee, Phys. Rev. D **72**, 014004 (2005).
 - [2] B.A. Kniehl, D.V. Vasin, and V.A. Seleev, Phys. Rev. D **73**, 074022 (2006).
 - [3] F. Abe *et al.* (CDF Collaboration), Phys. Rev. Lett. **79**, 578 (1997).
 - [4] χ_{cJ} will represent $\chi_{c1}(1P)$ or $\chi_{c2}(1P)$ mesons.
 - [5] V. Koreshev *et al.*, Phys. Rev. Lett. **77**, 4294 (1996); T. Alexopoulos *et al.* (E771 Collaboration), Phys. Rev. D **62**, 032006 (2000); T. Affolder *et al.* (CDF Collaboration), Phys. Rev. Lett. **86**, 3963 (2001).
 - [6] N. Brambilla *et al.*, hep-ph/0412158.
 - [7] W.-M. Yao *et al.* (Particle Data Group), J. Phys. G **33**, 1 (2006).
 - [8] D. Acosta *et al.* (CDF Collaboration), Phys. Rev. D **71**, 032001 (2005).
 - [9] D. Amidei *et al.*, Nucl. Instrum. Methods **350**, 73 (1994); F. Abe *et al.* (CDF Collaboration), Phys. Rev. D **50**, 2966 (1994).
 - [10] The pseudorapidity η is defined as $\eta \equiv -\ln(\tan(\theta/2))$, where θ is the angle between the particle momentum and the proton beam direction.
 - [11] B. Rossi and K. Greisen, Rev. Mod. Phys. **13**, 240 (1941).
 - [12] F. Abe *et al.* (CDF Collaboration), Phys. Rev. Lett. **79**, 573 (1997).
 - [13] R. S. Galik, B. K. Heltsley, and H. Mahlke, hep-ex/0608056.

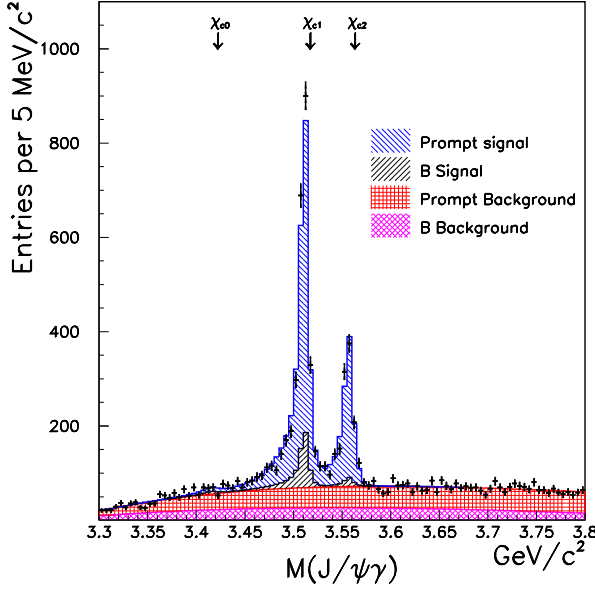


FIG. 1: The $J/\psi\gamma$ mass distribution (points) with the projection of the likelihood fit overlaid on the data. The masses of the χ_{cJ} mesons and the contributions of the signal and background components are indicated.

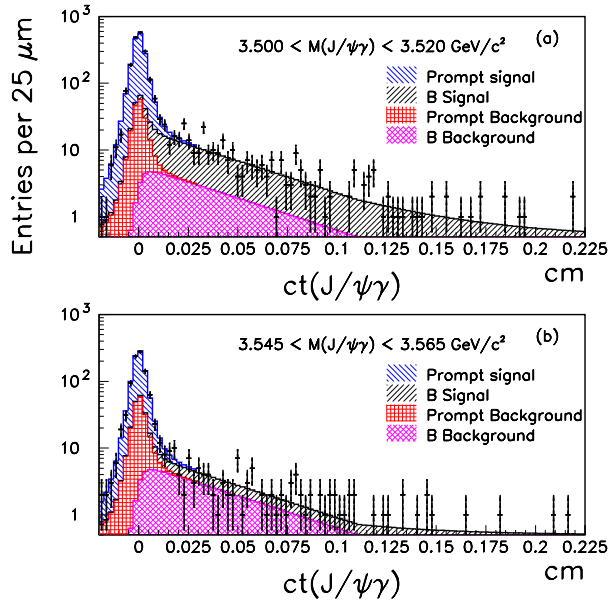


FIG. 2: The ct distribution (points) for events in the χ_{c1} (a) and χ_{c2} (b) mass ranges. The projection of the fit is overlaid on the data, with the contribution of each signal and background component indicated.